

Heavy flavour production in DGLAP improved saturation model

K. Golec-Biernat*

Institute of Nuclear Physics, Polish Academy of Sciences, Cracow, Poland

Institute of Physics, University of Rzeszów, Rzeszów, Poland

S. Sapeta†

M. Smoluchowski Institute of Physics, Jagellonian University, Cracow, Poland

(November 8, 2021)

Abstract

The charm and beauty quark production in deep inelastic scattering at low values of the Bjorken variable x is considered in the DGLAP improved saturation model. After fitting parameters of the model to the structure function F_2 , the heavy quark contributions $F_2^{c\bar{c}}$ and $F_2^{b\bar{b}}$ are predicted. A good description of the data is found. Predictions for the longitudinal structure function F_L and the diffractive structure function F_2^D are also presented.

*e-mail: golec@ifj.edu.pl

†e-mail: sapeta@th.if.uj.edu.pl

1 Introduction

Among the color dipole models of deep inelastic scattering at small values of the Bjorken variable x , the saturation model [1,2] (GBW model) turned out to be especially successful. It was able to describe both the low x structure function F_2 and the diffractive structure function F_2^D measured at HERA. From the theoretical side, the model has attracted a lot of attention since it grasps essential elements of parton saturation [3–5] incorporated in a relatively simple way. In particular, geometric scaling in DIS was predicted as a consequence of the assumptions on the saturation scale and scaling behaviour of the dipole cross section (which is a crucial element of the dipole models) [6]. With the advent of more precise HERA data [7–9], the GBW model needed improvement in order to provide better description of F_2 at large values of the photon virtuality ($Q^2 > 20 \text{ GeV}^2$). This was done by Bartels, Golec-Biernat and Kowalski (BGK) by incorporating into the saturation model a proper gluon density evolving according to the DGLAP evolution equations [10]. This modification improves the small- r part of the dipole cross section.

In the GBW saturation model the heavy quark contribution to F_2 was considered in the form of the $c\bar{c}$ pair production. This element, however, is missing in the BGK improvement. The recent data from HERA [11–13] shows that the heavy quark contribution is of the size up to 30% and can by no means be neglected. Thus, the main goal of this analysis is to take into account heavy quark production in the DGLAP improved saturation model and confront it with the recent data. This analysis does not introduce new parameters to those already present. Once the parameters of the dipole cross section are determined from a fit to the total structure function F_2 , they can be used to *predict* the charm and beauty contributions $F_2^{c\bar{c}}$ and $F_2^{b\bar{b}}$, which are not fitted separately. In addition, the longitudinal structure function F_L and the diffractive structure function F_2^D can also be predicted.

It should be stressed that other dipole models are also successful in the description of the DIS data. These include the model of Forshaw and Shaw [14–16] based on the Regge-like ideas combined with the idea of saturation, the model of Iancu, Itakura and Munier [17] closely related to the theory of the color glass condensate [18–25] and the model of McDermott, Frankfurt, Guzey and Strikman [26] which is close in spirit to our analysis. Quite recently, a new analysis of Kowalski, Motyka and Watt [27] appeared which addresses a very important problem of the impact parameter dependence of the dipole scattering amplitude. For more details on these models see recent review [28].

The outline of this paper is as follows. In Section 2 we recall the main features of the BGK saturation model. In Section 3 we describe fits with heavy flavours to the data on F_2 from HERA. In Section 4 we discuss main features of parton saturation, namely the critical line and saturation scale. Based on the results of the fits, in Section 5 we predict the charm and beauty contributions to F_2 and the longitudinal structure function. In Section 6 we discuss the diffractive structure function. Finally, conclusions are presented in Section 7.

2 The BGK saturation model

In the dipole picture of DIS at small values of x [29–33], the virtual photon–proton scattering cross sections $\sigma_{T,L}^{\gamma^*p}$ from transverse (T) and longitudinal (L) photons are given as a convolution

of the photon wave functions $\psi_{T,L}$ and the dipole cross section $\hat{\sigma}$,

$$\sigma_{T,L}^{\gamma^*p}(x, Q^2) = \sum_{f=1}^{N_f} \int d^2r dz |\psi_{T,L}(r, z, Q^2; m_f, e_f)|^2 \hat{\sigma}(x, r), \quad (1)$$

where f denotes flavour of the quark–antiquark pairs (dipoles) interacting with the proton (m_f and e_f are quark mass and electric charge, respectively). The integration is performed over the $q\bar{q}$ transverse separation vector r and the light-cone momentum fraction of the virtual photon z carried by the quark or antiquark. The proton structure function F_2 is proportional to the sum of the two cross sections

$$F_2 = \frac{Q^2}{4\pi^2\alpha_{em}} (\sigma_T^{\gamma^*p} + \sigma_L^{\gamma^*p}). \quad (2)$$

In the BGK model [10] the dipole cross section was assumed in the form

$$\hat{\sigma}(x, r) = \sigma_0 \left\{ 1 - \exp\left(-\frac{\pi^2 r^2 \alpha_s(\mu^2) xg(x, \mu^2)}{3\sigma_0}\right) \right\}, \quad (3)$$

which recovers the well known result of perturbative QCD [34] that for small dipole sizes the dipole cross section is proportional to the gluon distribution $g(x, \mu^2)$ with the scale $\mu^2 \sim 1/r^2$. Indeed, expanding (3) in powers of r^2 , we find to the first order

$$\hat{\sigma}(x, r) \simeq \frac{\pi^2}{3} r^2 \alpha_s xg(x, \mu^2). \quad (4)$$

The feature that $\hat{\sigma}(x, r)$ vanishes in the limit $r \rightarrow 0$ is called colour transparency and results from gauge invariance of QCD. The gluon distribution evolves with the scale according to the leading order DGLAP evolution equations. Since the model is applied in the low x region, quarks are neglected in the evolution. Inspired by the MRST parametrisation [35], the initial gluon distribution for the DGLAP evolution is taken in the form with two parameters, A_g and λ_g , to be determined from fits to data

$$xg(x, Q_0^2) = A_g x^{\lambda_g} (1-x)^{5.6}. \quad (5)$$

The initial scale Q_0^2 is conventionally set to 1 GeV²

The behaviour of the dipole cross section (3) at large r has not been changed with respect to the GBW model in which the dipole cross section saturates at the maximal value σ_0 (also to be determined from fits to data). This key assumption is in agreement with unitarity of the cross section σ^{γ^*p} . The large dipole sizes, however, are the cause of troubles for the scale of the gluon distribution in Eq. (3) since μ may become smaller than Λ_{QCD} . In order to avoid this we freeze the scale at some minimal value $\mu_0 \gg \Lambda_{\text{QCD}}$. Thus we assume that

$$\mu^2 = \frac{C}{r^2} + \mu_0^2, \quad (6)$$

which introduces two additional parameters, C and μ_0^2 , to be found from fits to data. For $r \rightarrow 0$ the presence of μ_0^2 becomes irrelevant and we recover the relation $\mu^2 \sim 1/r^2$.

On the whole, the BGK model has five parameters to be fitted: the dipole cross section bound σ_0 and the four parameters of the gluon distribution: A_g , λ_g , C and μ_0^2 . In comparison to the GBW saturation model, there are two new parameters introduced by the scale (6).

3 Fit description

We performed fits with the charm and beauty contributions in the sum in Eq. (1) using recent data on the proton structure function F_2 from H1 [7] and ZEUS [8,9]. We considered only the data points with $x \leq 0.01$ and $Q^2 \geq 0.04 \text{ GeV}^2$. The number of experimental points in such a case was equal to 288. The statistical and systematic errors were added in quadrature. Moreover, the H1 data were multiplied by a factor 1.05 to account for slightly different normalisation of the H1 and ZEUS data sets. Similarly to the analyses [1,10], we also modified the argument in the dipole cross section $\hat{\sigma}(x, r)$ in the heavy flavour contributions,

$$x \rightarrow x \left(1 + \frac{4m_f^2}{Q^2} \right) = \frac{Q^2 + 4m_f^2}{Q^2 + W^2}, \quad (7)$$

where W is invariant energy of the γ^*p system. This modification takes into account that the heavy quark masses play the role of the hard scale when $Q^2 \ll m_{c,b}^2$.

We took typical values of the heavy quark masses, $m_c = 1.3 \text{ GeV}$ and $m_b = 5.0 \text{ GeV}$, but the light quarks stayed massless. Therefore, we excluded the photoproduction point $Q^2 = 0$ from considerations since in the dipole models $\sigma^{\gamma p}$ depends logarithmically on the quark mass in the limit $Q^2 \rightarrow 0$. A comment is in order at this point. We performed preliminary fits with the light quark mass $m_q = 140 \text{ MeV}$ taken from [1]. However, we did not find the value of the photoproduction cross section measured at HERA ($174 \mu\text{b}$) [36]. Thus the description of photoproduction would require fine-tuning of the light quark mass in the region where perturbative QCD, which is the basis of the dipole models, is not valid. Nevertheless, in the case of the heavy flavour production, when the quark mass is the hard scale, the predictions for $Q^2 = 0$ could be done.

Before we present the results of our fits, let us mention that the GBW model with heavy flavours fitted to the new data [7–9] gives $\chi^2/\text{ndf} = 2.32$. As it has already been pointed out in [10], this rather poor fit quality results from the lack of the proper DGLAP evolution of the gluon distribution in the GBW model.

We performed two fits with the dipole cross section (3), taking into account the charm and beauty contribution in addition to the three light quarks. In the first fit only charm was considered while in the second one both heavy flavours were present. We set the number of active flavours in α_s to 4 and 5, respectively and the value of $\Lambda_{\text{QCD}} = 300 \text{ MeV}$ in both cases. The fit results for the five parameters of the model, σ_0 , A , λ_g , C and μ_0^2 , are presented in Table 1. In the last row we recall from [10] the parameters of the BGK fit with the light quarks only.

As we see, the value of χ^2/ndf is still good for the fits with heavy flavours. The gluon parameters differ significantly from the light quark fit. In particular, the power λ_g is negative which means that the initial gluon distribution (5) grows with decreasing x , in contrast to the fit with light quarks only when the gluon distribution is valence-like (λ_g is positive). With the found gluon density, the total proton momentum fraction carried by gluons is around 25% at the initial scale $Q_0^2 = 1 \text{ GeV}^2$.

In Fig. 1 we show the comparison of the dipole cross sections from the present analysis with heavy quarks (solid lines) and the BGK analysis [10] with light quarks only (dashed lines). The effect of heavy quarks is seen in the shift of the dipole cross section towards larger values of r , which means that for a given dipole size saturation occurs at lower x (higher energy). This effect was also observed in the GBW analysis [1].

	σ_0 [mb]	A_g	λ_g	C	μ_0^2	χ^2/ndf
light + c + b	22.7	1.23	- 0.080	0.35	1.60	1.16
light + c	22.4	1.35	- 0.079	0.38	1.73	1.06
light	23.8	13.71	0.41	11.10	0.52	0.97

Table 1: The parameters of our fits with heavy quarks to the F_2 data. The results of the BGK fit from [10] with massless light quarks only are given for the reference in the last row.

It should also be mentioned that the presence of heavy quarks in the DGLAP improved model cures the pathological behaviour of the dipole cross section found in [10] in the fit with massless quarks (FIT 2). This is why we choose the BGK fit with massive light quarks (FIT 1) for the comparison in Fig. 1.

4 Critical line and saturation scale

The shift of the dipole cross section towards larger values of r has direct impact on the position of the critical line which marks the transition to the saturation region in the (x, Q^2) -plane. The line is defined by the condition

$$\hat{\sigma}_0(x, \bar{r}) = a \sigma_0, \quad (8)$$

with the constant a of the order of unity and the dipole size taken at its characteristic value $\bar{r} = 2/Q$. In the GBW and BGK analyses the critical line was defined by the condition that the argument of the exponent in the dipole cross section equals 1, which corresponds to $a = 1 - e^{-1} \approx 0.63$. With the form (3), the following implicit relation between x and Q^2 is found in such a case

$$\frac{4\pi^2}{3\sigma_0 Q^2} \alpha_s(\mu^2) x g(x, \mu^2) = 1, \quad (9)$$

where the scale $\mu^2 = CQ^2/4 + \mu_0^2$. This equation can be solved numerically to obtain the critical line shown in Fig. 3 as the solid line. The saturation effects are important to the left of this line. For the comparison, we also show the critical lines from the BGK and GBW analysis with light quarks only. We observe that the presence of heavy quarks shifts the critical line towards smaller values of Q^2 . This means that for a given Q^2 we need lower x in order to stay in the domain where the saturation effects are important. In other words, heavy quarks make saturation more difficult to observe at present and also future colliders, which is indicated in Fig. 3 by the acceptance regions of HERA and the LHC.

An important element of the description of parton saturation in the GBW model [1] was the saturation scale, $Q_s(x) = Q_{s0} x^{-\lambda}$, built in the dipole cross section

$$\hat{\sigma}(x, r) = \sigma_0 \left\{ 1 - \exp\left(-\frac{1}{4}r^2 Q_s^2(x)\right) \right\}. \quad (10)$$

This form of the dipole cross section features the scaling behaviour, $\hat{\sigma}(x, r) = \hat{\sigma}(rQ_s(x))$, which for massless quarks leads to geometric scaling of the total cross section,

$$\sigma^{\gamma^*p} = \sigma^{\gamma^*p}(Q^2/Q_s^2(x)), \quad (11)$$

found to a good accuracy in the small x HERA data [6, 37]. Notice that the critical line in the GBW model is defined as a simple condition: $Q^2 = Q_s^2(x)$.

The BGK modification of the saturation model seems to abandon these important elements. Fortunately, this is not the case since in the fits with heavy flavours the value of C in the gluon scale (6) is small whereas $\mu_0^2 \approx 1.6 \text{ GeV}^2$ is relatively large. It means that for not too small r , the dipole cross sections (3) effectively features the scaling at large values of r with the saturation scale proportional to the gluon distribution at the scale μ_0^2

$$Q_s^2(x) \simeq \frac{4\pi^2}{3\sigma_0} \alpha_s(\mu_0^2) xg(x, \mu_0^2). \quad (12)$$

Indeed, as we see in Fig. 2, which shows the dipole cross section as a function of the scaling variable $r^2 Q_s^2(x)$, geometric scaling is preserved for moderate values of r . It is broken, however, for small dipole sizes due to the DGLAP evolution of the gluon in the dipole cross section.

It is important to notice that from the theoretical perspective, based on the theory of the color glass condensate (see [38] for most recent review), our considerations are confined to the mean field approximation which neglects the effects of fluctuations in the number of color dipoles in the proton wave function. These effects are important in the low density region of dipoles with very small sizes. For sufficiently small x (large rapidity $Y = \ln(1/x)$), the fluctuations wash out geometric scaling leading to *diffusive scaling* [39–46]. The DIS cross sections in this case become functions of the variable $\ln[Q^2/Q_s^2(Y)]/\sqrt{DY}$ rather than $Q^2/Q_s^2(Y)$. The discussion of the new type of scaling is, however, beyond the scope of the presented analysis.

5 Predictions for inclusive structure functions

Once the parameters of the dipole cross sections (3) are determined from the fit to the F_2 data, various inclusive structure functions can be predicted. In particular, the heavy quark contributions, $F_2^{c\bar{c}}$ and $F_2^{b\bar{b}}$, can be found from the flavour decomposition in Eq. (1)

$$F_2 = F_2^{light} + F_2^{c\bar{c}} + F_2^{b\bar{b}}. \quad (13)$$

The dependence on flavour comes through electric charge e_f and mass m_f in the photon wave functions $\psi_{T,L}$. For heavy quarks the mass also enters the dipole cross section through the modified value of the Bjorken variable (7). This allows to compute the $c\bar{c}$ and $b\bar{b}$ photoproduction cross sections. For the HERA energy $W = 209 \text{ GeV}$, we found $19.3 \mu\text{b}$ and $0.7 \mu\text{b}$, respectively. To our astonishment, substituting the mass $m_q = 140 \text{ MeV}$ for the three light quarks to the formula for $\sigma^{\gamma p}$ and performing then the photoproduction limit $Q^2 \rightarrow 0$, we found $177 \mu\text{b}$ which agrees with the measured value $174 \mu\text{b}$ up to the experimental errors.

The predictions for $F_2^{c\bar{c}}$ and $F_2^{b\bar{b}}$ computed with the parameters from the first line of Table 1 are presented as the solid lines in Figs. 4 and 5, respectively. For the comparison, we present the predictions of the GBW model without the DGLAP modification (dashed lines). We see very good agreement with the data from HERA, both in the normalisation and the slope in x , in contrast to the GBW results which overshoot the data at large values of Q^2 . Thus, the presence of the DGLAP evolution in the BGK model is crucial for the correct predictions at large Q^2 . This can be understood by analysing the contribution of different dipole sizes to the heavy quark structure functions. For $Q^2 \gg 4m_f^2$, they are mostly sensitive to the small- r part of the dipole cross section ($r \approx 2/Q$) which is strongly modified by the DGLAP improvement.

In Figure 6 we present the longitudinal structure function from our analysis (solid line), plotted against Q^2 for $W = 276 \text{ GeV}$. The experimental points represent the H1 estimations of

F_L [7, 47, 48]. Reasonable agreement is found, however, the estimation errors are too large to draw firm conclusions. We also show the charm and beauty contribution to F_L (dashed line). We observe that in our analysis heavy quarks are important for large values of Q^2 while for $Q^2 < 10 \text{ GeV}^2$ they may safely be neglected.

6 DIS diffraction

Deep inelastic diffraction is an important test of the dipole models [2, 49, 50]. The dipole cross section from the inclusive analysis can be applied to the description of the diffractive structure function. Following the approach presented in [2], the diffractive structure function is the sum of three contributions

$$F_2^{D(3)}(x_{\mathbb{P}}, \beta, Q^2) = F_T^{q\bar{q}} + F_L^{q\bar{q}} + F_T^{q\bar{q}g}, \quad (14)$$

which correspond to the diffractive systems composed of the $q\bar{q}$ and $q\bar{q}g$ dipoles with invariant mass M , produced by the transversely and longitudinally polarised virtual photons. Their interaction with the proton is described by the dipole cross section $\hat{\sigma}(x_{\mathbb{P}}, r)$. Note that

$$x_{\mathbb{P}} = \frac{Q^2 + M^2}{Q^2 + W^2} = \frac{x}{\beta} \quad (15)$$

is substituted instead of the Bjorken x as an argument of $\hat{\sigma}$. The longitudinal component $F_L^{q\bar{q}g}$ is suppressed by $1/Q^2$ and is negligible in the region of small values of $\beta = Q^2/(Q^2 + M^2)$, *i.e.* for large diffractive masses $M^2 \gg Q^2$, where the transverse $q\bar{q}g$ component dominates.

The $q\bar{q}g$ diffractive amplitude was computed in [2] in the two-gluon exchange approximation with strong ordering of transverse momenta of the $q\bar{q}$ pair and the gluon. Each contribution is proportional to the inverse of the diffractive slope B_D for which we took the experimental value $B_D = 6 \text{ GeV}^{-2}$. In addition, the $q\bar{q}g$ component is proportional to the strong coupling which we took a typical $\alpha_s = 0.2$. However, this is not quite clear which value of α_s should be used, thus the normalisation of this term is rather uncertain.

In Fig. 7 we show the comparison of the diffractive structure function $F_2^{D(3)}$ computed in our analysis with the data from H1 [51, 52] and ZEUS [53, 54]. However, these data are obtained for different upper limits on the mass of the proton dissociation system, $M_Y < 2.3 \text{ GeV}$ for ZEUS and $M_Y < 1.6 \text{ GeV}$ for H1. To account for this, the ZEUS data in Fig. 7 is multiplied by the global factor 0.86 in accordance with [51]. At the same time we multiplied our predictions for the nondissociated proton by 1.23. This number, taken from [51], is the correction factor which takes into account the proton dissociation up to the mass $M_Y < 1.6 \text{ GeV}$. Thus, both the data and the theoretical predictions are normalised to the same experimental situation. The parameters from the first line of Table 1 were used in the dipole cross section for the computation of $F_2^{D(3)}$. As we see from Fig. 7, reasonable agreement with the data is found.

In contrast to the inclusive case, the $c\bar{c}$ and $b\bar{b}$ contributions to the diffractive structure function are negligible due to the phase space restrictions for the diffractive system. The analysis of the diffractive $c\bar{c}g$ production, however, deserves more detailed considerations based on the seminal work [55, 56].

7 Conclusions

We discussed the production of the charm and beauty flavours in the DGLAP improved saturation model [10]. We fitted the parameters of the model to the recent F_2 data from HERA, taking into account the heavy quark contributions in the theoretical formula for F_2 . We found a good quality fit with χ^2/ndf close to unity. Thus we conclude that the successful description of the inclusive F_2 data at low x which was found for the BGK model with light quarks is preserved when heavy flavours are considered. There are, however, some differences introduced by heavy quarks. First of all, the parameters vary significantly for the models with and without heavy flavours. This results in the shift of the dipole cross section towards larger values of the dipole sizes r with respect to the light quark case. As a consequence, the critical line in (x, Q^2) -plane moves in the direction of smaller values of Q^2 which makes saturation more difficult to observe.

The new predictions provided by our analysis concern the charm and beauty structure functions $F_2^{c\bar{c}}$ and $F_2^{b\bar{b}}$. We found very good agreement with H1 and ZEUS data in all Q^2 bins. The significant improvement of the slope in x for high Q^2 with respect the GBW model is attributed to the DGLAP evolution.

Other structure functions were also determined. For the longitudinal structure function F_L , we found agreement with the H1 estimations. However, large estimation errors prevent from making more precise statement. The comparison with direct measurements, which are planned by H1 and ZEUS collaborations, will be particularly interesting. For the diffractive structure function $F_2^{D(3)}$, we observe reasonable agreement with the H1 and ZEUS data after a proper renormalisation of the data points.

Finally, we discussed the issues related to the essential features of parton saturation like the saturation scale and geometric scaling. We showed that saturation scale is effectively present in the DGLAP improved model being related to the gluon distribution at the frozen value of the factorisation scale μ_0^2 .

Acknowledgments

We thank the Theory Group members at Ecole Polytechnique where this analysis was completed for their warm hospitality and Laurent Schoeffel for helping us to prepare Fig. 7. This research has been partly supported by the MEiN research grants: No. 1 P03B 028 28 (2005-08), No. N202 048 31/2647 (2006-08) and by the French–Polish scientific agreement Polonium.

References

- [1] K. Golec-Biernat and M. Wusthoff, Phys. Rev. **D59**, 014017 (1999), [hep-ph/9807513].
- [2] K. Golec-Biernat and M. Wusthoff, Phys. Rev. **D60**, 114023 (1999), [hep-ph/9903358].
- [3] L. V. Gribov, E. M. Levin and M. G. Ryskin, Phys. Rept. **100**, 1 (1983).
- [4] A. H. Mueller and J.-w. Qiu, Nucl. Phys. **B268**, 427 (1986).
- [5] A. H. Mueller, Nucl. Phys. **B335**, 115 (1990).
- [6] A. M. Stasto, K. Golec-Biernat and J. Kwiecinski, Phys. Rev. Lett. **86**, 596 (2001), [hep-ph/0007192].

- [7] H1, C. Adloff *et al.*, Eur. Phys. J. **C21**, 33 (2001), [hep-ex/0012053].
- [8] ZEUS, S. Chekanov *et al.*, Eur. Phys. J. **C21**, 443 (2001), [hep-ex/0105090].
- [9] ZEUS, J. Breitweg *et al.*, Phys. Lett. **B487**, 53 (2000), [hep-ex/0005018].
- [10] J. Bartels, K. Golec-Biernat and H. Kowalski, Phys. Rev. **D66**, 014001 (2002), [hep-ph/0203258].
- [11] H1, C. Adloff *et al.*, Phys. Lett. **B528**, 199 (2002), [hep-ex/0108039].
- [12] H1, A. Aktas *et al.*, Eur. Phys. J. **C40**, 349 (2005), [hep-ex/0411046].
- [13] ZEUS, S. Chekanov *et al.*, Phys. Rev. **D69**, 012004 (2004), [hep-ex/0308068].
- [14] J. R. Forshaw, G. Kerley and G. Shaw, Phys. Rev. **D60**, 074012 (1999), [hep-ph/9903341].
- [15] J. R. Forshaw, G. R. Kerley and G. Shaw, Nucl. Phys. **A675**, 80c (2000), [hep-ph/9910251].
- [16] J. R. Forshaw and G. Shaw, JHEP **12**, 052 (2004), [hep-ph/0411337].
- [17] E. Iancu, K. Itakura and S. Munier, Phys. Lett. **B590**, 199 (2004), [hep-ph/0310338].
- [18] L. D. McLerran and R. Venugopalan, Phys. Rev. **D49**, 2233 (1994), [hep-ph/9309289].
- [19] L. D. McLerran and R. Venugopalan, Phys. Rev. **D49**, 3352 (1994), [hep-ph/9311205].
- [20] J. Jalilian-Marian, A. Kovner, A. Leonidov and H. Weigert, Phys. Rev. **D59**, 014014 (1999), [hep-ph/9706377].
- [21] J. Jalilian-Marian, A. Kovner and H. Weigert, Phys. Rev. **D59**, 014015 (1999), [hep-ph/9709432].
- [22] H. Weigert, Nucl. Phys. **A703**, 823 (2002), [hep-ph/0004044].
- [23] E. Iancu, A. Leonidov and L. D. McLerran, Nucl. Phys. **A692**, 583 (2001), [hep-ph/0011241].
- [24] E. Ferreiro, E. Iancu, A. Leonidov and L. McLerran, Nucl. Phys. **A703**, 489 (2002), [hep-ph/0109115].
- [25] E. Iancu, A. Leonidov and L. D. McLerran, Phys. Lett. **B510**, 133 (2001), [hep-ph/0102009].
- [26] M. McDermott, L. Frankfurt, V. Guzey and M. Strikman, Eur. Phys. J. **C16**, 641 (2000), [hep-ph/9912547].
- [27] H. Kowalski, L. Motyka and G. Watt, hep-ph/0606272.
- [28] J. R. Forshaw, R. Sandapen and G. Shaw, hep-ph/0608161.
- [29] N. N. Nikolaev and B. G. Zakharov, Z. Phys. **C49**, 607 (1991).
- [30] N. Nikolaev and B. G. Zakharov, Z. Phys. **C53**, 331 (1992).
- [31] A. H. Mueller, Nucl. Phys. **B415**, 373 (1994).
- [32] A. H. Mueller and B. Patel, Nucl. Phys. **B425**, 471 (1994), [hep-ph/9403256].

- [33] A. H. Mueller, Nucl. Phys. **B437**, 107 (1995), [hep-ph/9408245].
- [34] L. Frankfurt, A. Radyushkin and M. Strikman, Phys. Rev. **D55**, 98 (1997), [hep-ph/9610274].
- [35] A. D. Martin, R. G. Roberts, W. J. Stirling and R. S. Thorne, Phys. Lett. **B531**, 216 (2002), [hep-ph/0201127].
- [36] ZEUS, S. Chekanov *et al.*, Nucl. Phys. **B627**, 3 (2002), [hep-ex/0202034].
- [37] C. Marquet and L. Schoeffel, hep-ph/0606079.
- [38] E. Iancu, hep-ph/0608086.
- [39] A. H. Mueller and A. I. Shoshi, Nucl. Phys. **B692**, 175 (2004), [hep-ph/0402193].
- [40] E. Iancu, A. H. Mueller and S. Munier, Phys. Lett. **B606**, 342 (2005), [hep-ph/0410018].
- [41] S. Munier, Nucl. Phys. **A755**, 622 (2005), [hep-ph/0501149].
- [42] G. Soyez, Phys. Rev. **D72**, 016007 (2005), [hep-ph/0504129].
- [43] R. Enberg, K. Golec-Biernat and S. Munier, Phys. Rev. **D72**, 074021 (2005), [hep-ph/0505101].
- [44] Y. Hatta, E. Iancu, C. Marquet, G. Soyez and D. N. Triantafyllopoulos, Nucl. Phys. **A773**, 95 (2006), [hep-ph/0601150].
- [45] E. Brunet, B. Derrida, A. H. Mueller and S. Munier, Phys. Rev. **E73**, 056126 (2006), [cond-mat/0512021].
- [46] C. Marquet, G. Soyez and B.-W. Xiao, Phys. Lett. **B639**, 635 (2006), [hep-ph/0606233].
- [47] H1, C. Adloff *et al.*, Eur. Phys. J. **C30**, 1 (2003), [hep-ex/0304003].
- [48] E. M. Lobodzinska, Acta Phys. Polon. **B35**, 223 (2004).
- [49] J. R. Forshaw, R. Sandapen and G. Shaw, Phys. Lett. **B594**, 283 (2004), [hep-ph/0404192].
- [50] S. Munier and A. Shoshi, Phys. Rev. **D69**, 074022 (2004), [hep-ph/0312022].
- [51] H1, hep-ex/0606004.
- [52] H1, hep-ex/0606003.
- [53] ZEUS, S. Chekanov *et al.*, Eur. Phys. J. **C38**, 43 (2004), [hep-ex/0408009].
- [54] ZEUS, S. Chekanov *et al.*, Nucl. Phys. **B713**, 3 (2005), [hep-ex/0501060].
- [55] M. Wusthoff and A. D. Martin, J. Phys. **G25**, R309 (1999), [hep-ph/9909362].
- [56] J. Bartels, H. Jung and A. Kyrrieleis, Eur. Phys. J. **C24**, 555 (2002), [hep-ph/0204269].
- [57] A. D. Martin, R. G. Roberts, W. J. Stirling and R. S. Thorne, Eur. Phys. J. **C14**, 133 (2000), [hep-ph/9907231].

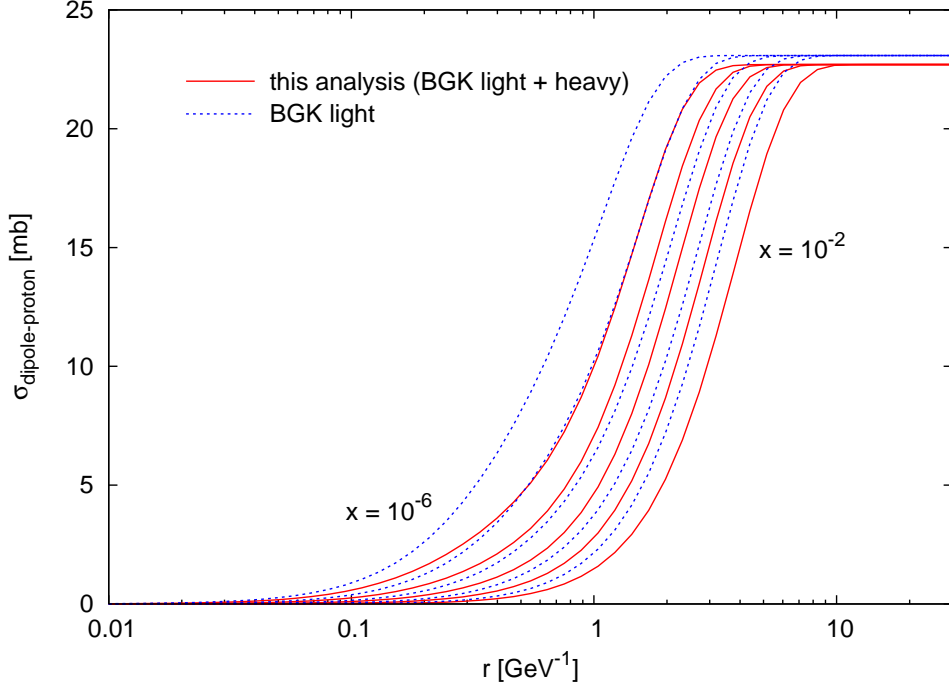


Figure 1: The dipole cross section in the BGK model with and without heavy quarks (solid and dashed lines, respectively) for $x = 10^{-2} \dots 10^{-6}$.

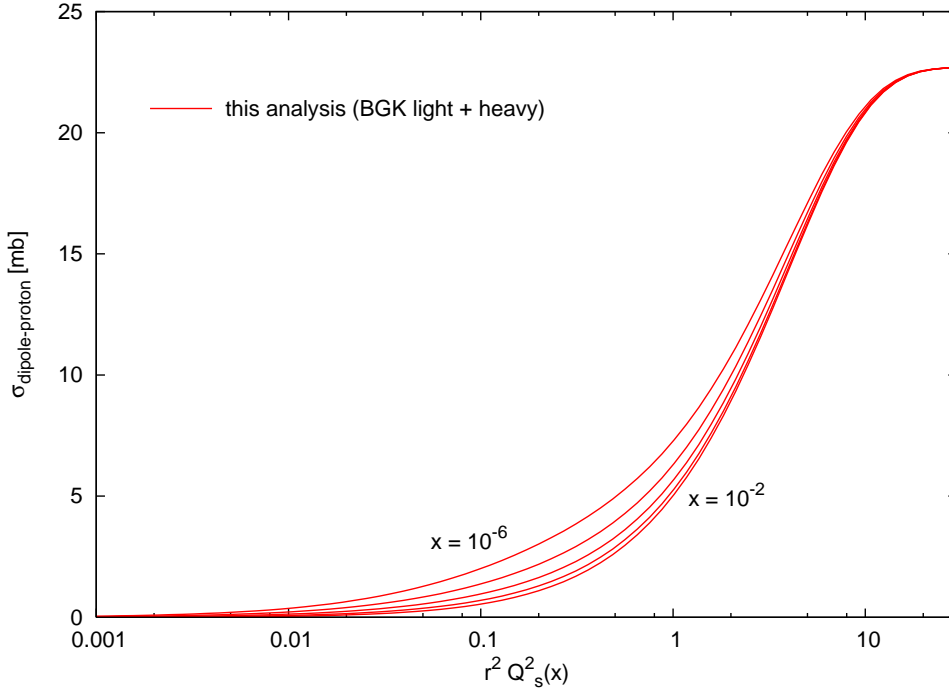


Figure 2: The dipole cross section in the BGK model with heavy quarks as a function of the scaling variable $r^2 Q_s^2(x)$ with the saturation scale given by Eq. (12). Geometric scaling is preserved for moderate dipole sizes, while it is broken for small values of r because of the DGLAP modification.

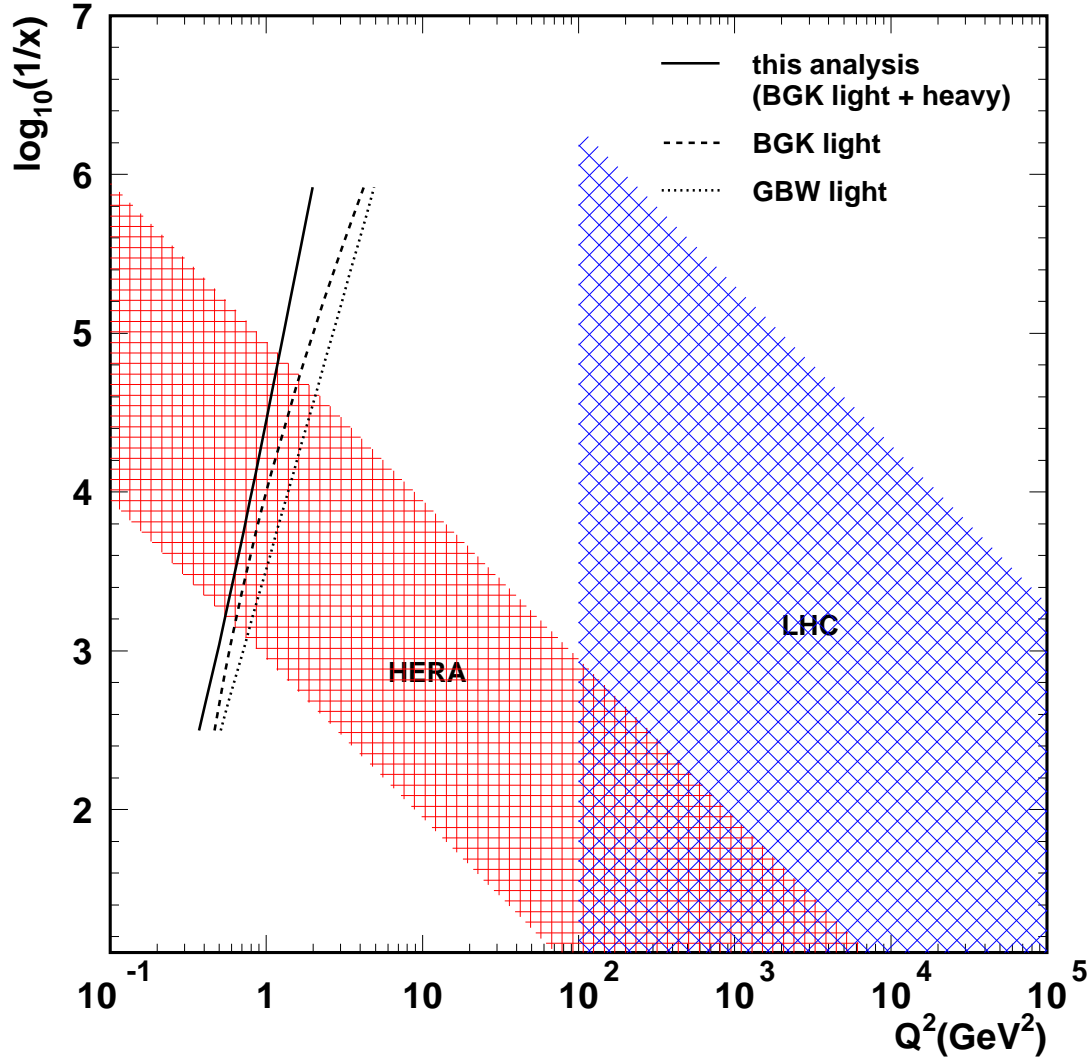


Figure 3: The critical line in the (x, Q^2) -plane from various saturation models indicating the position of the saturation region (to the left of these lines). The shaded areas show the acceptance regions of HERA and the LHC. The latter region corresponds to the production of an object with the minimal mass squared $Q^2 = 100 \text{ GeV}^2$ [57].

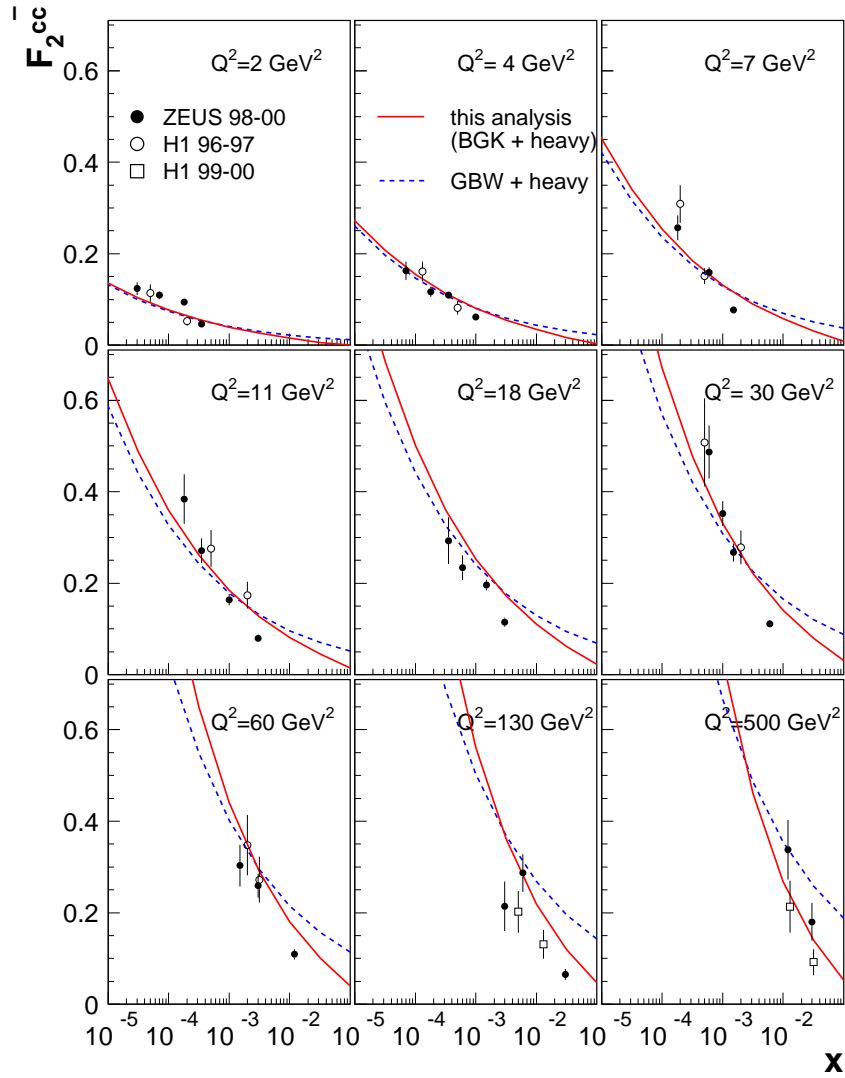


Figure 4: Predictions for the charm structure function F_2^{cc} in the BGK model with heavy quarks (solid lines). The predictions in the GBW model [1] are shown for reference (dashed lines).

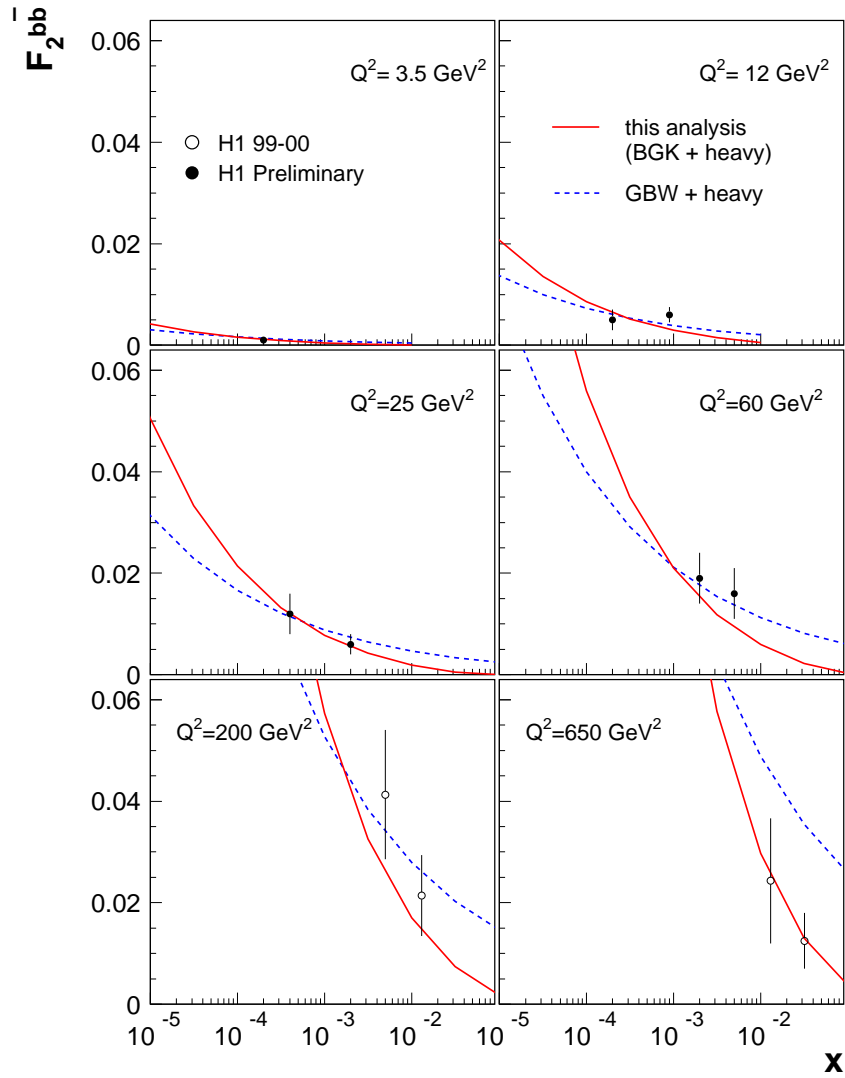


Figure 5: Predictions for the beauty structure function F_2^{bb} in the BGK model with heavy quarks (solid lines). The predictions in the GBW model [1] are shown for reference (dashed lines).

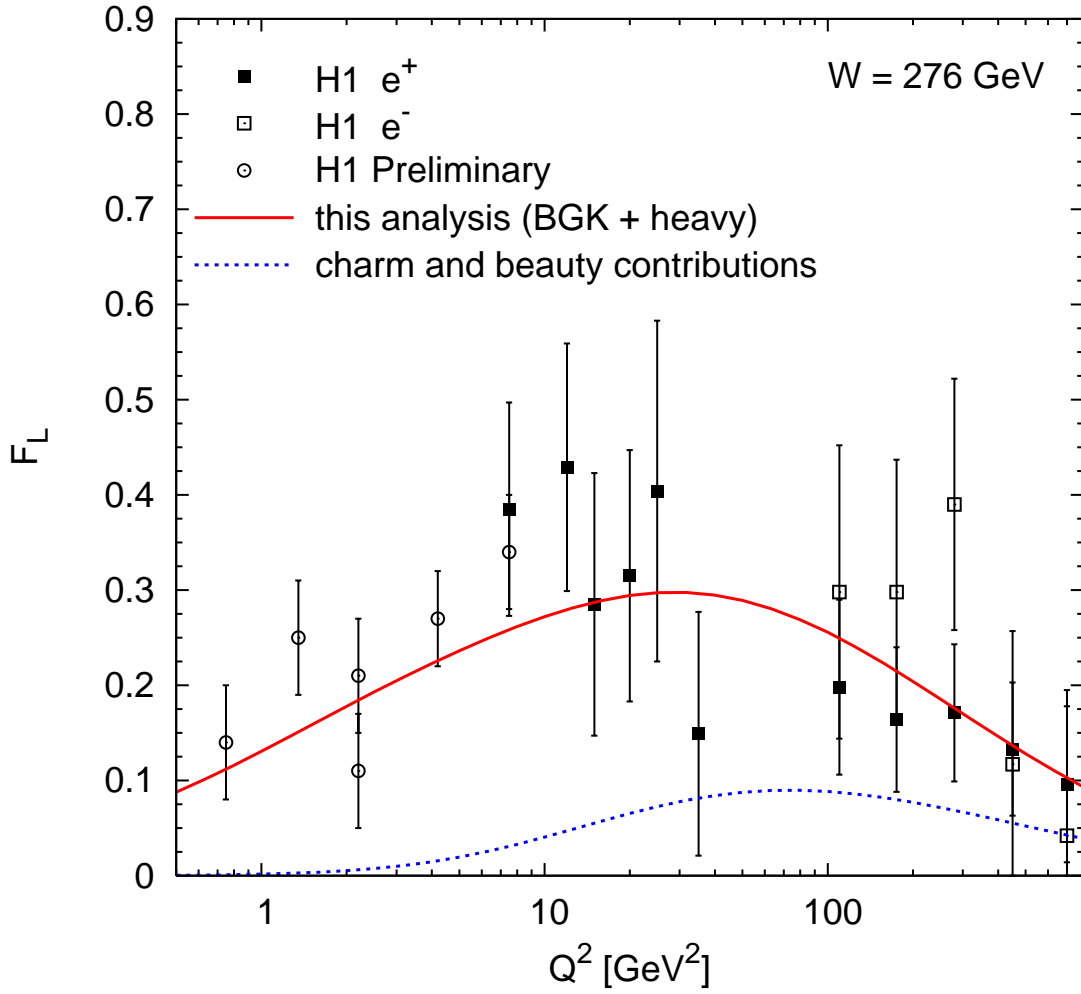


Figure 6: The longitudinal structure function predicted in the BGK model with heavy quarks together with the H1 estimations for various Q^2 at constant energy $W = 276$ GeV.

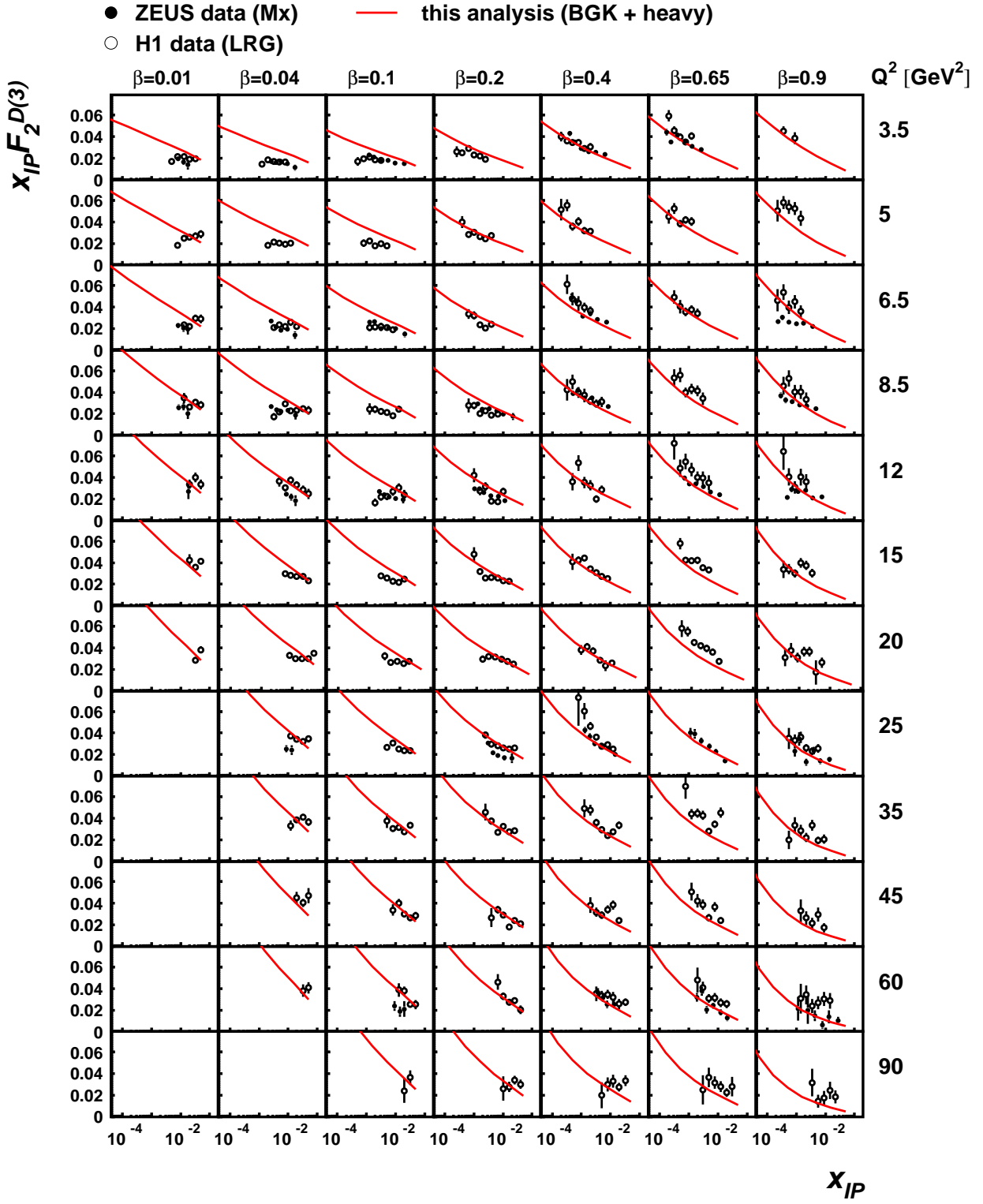


Figure 7: The diffractive structure function $x_P F_2^{D(3)}(x_P, \beta, Q^2)$. The predictions of our analysis with heavy quarks are compared with the recent H1 and ZEUS data.